Atmospheric Environment 331 (2024) 120538

Contents lists available at ScienceDirect

Atmospheric Environment

journal homepage: www.elsevier.com/locate/atmosenv

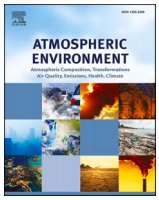

Measurements of particulate methanesulfonic acid above the remote Arctic Ocean using a high resolution aerosol mass spectrometer

Yangmei Zhang [a,*], Junying Sun [a], Xiaojing Shen [a], Vipul Lal Chandani [b], Mao Du [b], Congbo Song [b,1], Yuqing Dai [b], Guoyuan Hu [c], Mingxi Yang [d], Gavin H. Tilstone [d], Tom Jordan [d], Giorgio Dall'Olmo [e], Quan Liu [a], Eiko Nemitz [f], Anna Callaghan [g], James Brean [b], Roberto Sommariva [b], David Beddows [b], Ben Langford [f], William Bloss [b], William Acton [b], Zongbo Shi [b,h]

[a] State Key Laboratory of Severe Weather/Key Laboratory of Atmospheric Chemistry of China Meteorological Administration, Chinese Academy of Meteorological Sciences, Beijing, 100081, PR China
[b] School of Geography Earth and Environmental Sciences, University of Birmingham, Birmingham, B15 2TT, UK
[c] School of Electronic Information, Wuhan University, Wuhan, 430070, Hubei Province, PR China
[d] Plymouth Marine Laboratory, Prospect Place, Plymouth, Devon, PL1 3DH, UK
[e] Istituto Nazionale di Oceanografia e di Geofisica Sperimentale – OGS, Sezione di Oceanografia, Borgo Grotta Gigante 42/c, 34010, Sgonico, Trieste, Italy
[f] UK Centre for Ecology & Hydrology, Bush Estate, Penicuik, EH26 0QB, UK
[g] Wolfson Atmospheric Chemistry Observatory (WACL), University of York, York, UK
[h] Anhui Institute of Optics and Fine Mechanics, Chinese Academy of Sciences, 231137, Hefei, PR China

HIGHLIGHTS

- A validated quantification method was employed to determine the particulate MSA mass concentration by HR-TOF-AMS.
- The OH-initiated pathway is an important mechanism for the conversion of DMS into MSA above the remote ocean.
- Mass ratio of MSA to nss-SO_4 presents temperature dependence during the whole cruise.

GRAPHICAL ABSTRACT

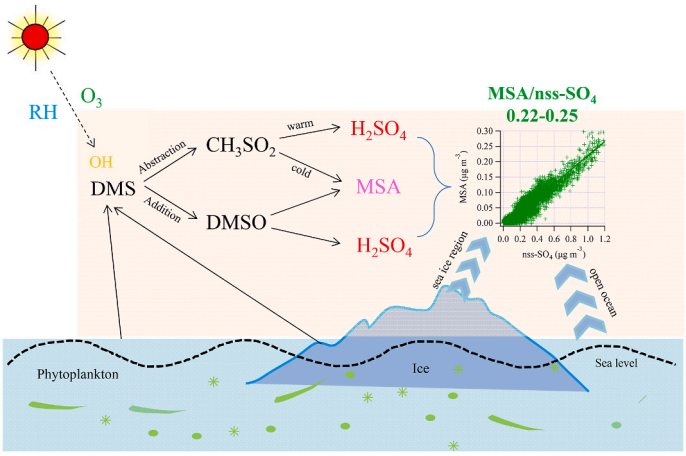

* Corresponding author.
E-mail addresses: ymzhang@cma.gov.cn (Y. Zhang), z.shi@bham.ac.uk (Z. Shi).
[1] Now at: National Centre for Atmospheric Science (NCAS), University of Manchester, Manchester M13 9PL, UK.

https://doi.org/10.1016/j.atmosenv.2024.120538
Received 17 November 2023; Received in revised form 10 April 2024; Accepted 25 April 2024
Available online 30 April 2024

ARTICLE INFO

Keywords:
MSA
Marine aerosol
Oxidation path
Reference MSA/nss-SO_4 value
HR-ToF-AMS

ABSTRACT

Methanesulfonic acid (MSA) is an important product from the oxidation of dimethyl sulfide (DMS), and thus is often used as a tracer for marine biogenic sources and secondary organic aerosol. MSA also contributes to aerosol mass and potentially to the formation of cloud condensation nuclei and new particles. However, measurements of MSA at high temporal resolution in the remote Arctic are scarce, which limits our understanding of its formation, climate change impact and regional transport. Here, we applied a validated quantification method to determine the mass concentration of MSA and non-sea salt sulfate (nss-SO_4) in $PM_{2.5}$ in the marine boundary layer, using a high resolution time-of-flight aerosol mass spectrometer (HR-ToF-AMS) during a research cruise to the Arctic and North Atlantic Ocean, between 55 °N and 68 °N (26th May to June 23, 2022). With this method, the concentrations of MSA in the remote Arctic marine boundary layer were determined for the first time. Results show that the average MSA concentration was 0.025 ± 0.03 μg m^{-3}, ranging from <0.01 to 0.32 μg m^{-3}. The lowest MSA level was found towards the northern leg of the cruise (near Sisimut (67 °N)) with air masses from sea ice over the northern polar region, and the highest MSA concentrations were observed over the Atlantic open ocean. The diurnal cycles of gas MSA, particulate MSA and nss-SO_4 peaked in the afternoon, about one hour later than that of peak of solar radiation, which suggests that photochemical process is an important mechanism for the conversion of DMS into MSA above the remote ocean. The mass ratio of MSA to nss-SO_4 (MSA/nss-SO_4) presents a temperature dependence, which indicates that the addition branching pathway favors MSA formation, while thermal decay of intermediate radicals could be a possible pathway for sulfate formation. Finally, we found that the MSA/nss-SO_4 ratio is around 0.22-0.25 in the remote northern marine atmosphere.

1. Introduction

Marine aerosol is an important part of the total natural aerosol in remote locations. It also has a significant impact on the global aerosol budget and climate (Ma et al., 2021; O'Dowd and Deleeuw, 2007; Ovadnevaite et al., 2014; Quinn et al., 2008). In general, marine aerosol particles consist of primary and secondary particles including sea salt generated from sea-air interaction and chemical products via atmospheric reactions of gases emitted by organisms in the ocean (Charlson et al., 1987). Dimethyl sulfide (DMS), a well-known biological gas emitted from marine phytoplankton, can be oxidized into sulfate and methane sulfonic acid (MSA). MSA is also suggested to play an important role in marine aerosol new particle formation (Dall'Osto et al., 2018; Hodshire et al., 2019; Ning and Zhang, 2022) as well as stratocumulus cloud formation over the remote ocean (Huang et al., 2015a). Local photochemical activities usually play a dominant role in marine MSA formation, while the aqueous phase processing enhances its condensation and coagulation (Chen et al., 2018). Bork et al. (2014) used the Atmospheric Cluster Dynamics Code kinetic model (McGrath et al., 2012; Olenius et al., 2013) to show that the presence of MSA could increase the molecular cluster formation rates by as much as an order of magnitude for the MSA–H_2SO_4–DMA (dimethylamine) system under atmospherically relevant MSA concentrations (Hodshire et al., 2019). The oxidation mechanism and the precursor of MSA, has been investigated in several studies using an extensive array of instrumentation (Hodshire et al., 2019; Hoffmann et al., 2016; Ning and Zhang, 2022; Shen et al., 2022; Stefels et al., 2007; Veresa et al., 2020). Chamber and flow-tube experiments, however, had difficulties in reproducing DMS oxidation under representative real atmospheric conditions. Measurements of MSA and its related species within the real atmosphere are therefore required to better understand the processes and mechanisms and thus improve the performance of atmospheric chemistry models.

MSA has previously been measured with a low time resolution, from several hours to days using offline methods. This prevents a mechanistic understanding of DMS chemistry and their impacts on new particle growth and cloud condensation nuclei formation. High resolution time-of-flight aerosol mass spectrometer (HR-ToF-AMS) is considered as one of the most widespread online instruments, measuring non-refractory components of submicron particles. Although MSA is not a typical compound (such as organics, sulfate, nitrate, ammonium and chloride) reported from AMS measurements, several studies have used HR-ToF-AMS to determine MSA mass concentration (Chen et al., 2019; Hodshire et al., 2019; Huang et al., 2015b, 2017, 2018; Ovadnevaite et al., 2014; Zorn et al., 2008). The response of the AMS to MSA however, is not fully characterized, and therefore, an independent quantification method needs to be used for each experiment.

Measurements of MSA over the marine atmosphere and continental regions have been made at several sites, such as Mace Head in Ireland (Ovadnevaite et al., 2014), Bermuda over North Atlantic (Savoie et al., 2002), Tenerife in Spain (Savoie et al., 2002), Barbados located in the Eastern Caribbean (Savoie et al., 2002), the Tropical Atlantic (van Pinxteren et al., 2015), South Atlantic (Lin et al., 2012), megacity Paris (Crippa et al., 2013), Coastal HongKong (Huang et al., 2015a) and the Arctic (Becagli et al., 2019). Most of these measurements focused on densely populated regions that are impacted by anthropogenic emission. Consequently, more detailed knowledge is needed on natural Arctic aerosol emissions, their evolution, transport and the effects on cloud microphysics (Schmale et al., 2021). The remote Arctic and North Atlantic Ocean, defined as latitudes >63 °N, is far from anthropogenic sources and is considered as an ideal place to study the natural marine atmosphere. The ratio of MSA to nss-SO_4 is an important indicator of both regional variations and anthropogenic perturbation in current and historical samples (Shen et al., 2022). It is also important to understand the changing natural aerosol baseline in the Arctic in response to warming and Arctic amplification (Schmale et al., 2021) and the resulting MSA/nss-SO_4 is essential to further our understanding of their roles in climate change (Shen et al., 2022). Up to now, MSA measurements carried out in the remote marine atmosphere are limited, and the mechanisms of MSA formation in the cold and clean marine boundary layer environment are poorly understood.

In this study, HR-ToF-AMS measurements of marine aerosol measurements were conducted on a ship-based cruise of the remote northern Atlantic Ocean, along the west side of Greenland (55 °N) and up to Davis Strait (between 63 °N and 68 °N) near sea ice area. Based on specific laboratory and field calibration, a validated method was used to quantify the MSA and nss-SO_4 mass concentration. The variation of MSA, nss-SO_4 mass concentration, and ratio of MSA to nss-SO_4 during the cruise were surveyed. The evolution of MSA and potential oxidation pathway of MSA and nss-SO_4 formation from DMS were discussed. Finally, from the ratio of MSA to nss-SO_4, together with back trajectory analysis, reference value of MSA/nss-SO_4 for remote marine atmosphere, the potential contributions of anthropogenic and natural marine sources were discussed.

2. Experiment and methods

2.1. Overview of observations during the DY151 research cruise

The DY151 research cruise on the *Royal Research Ship (RRS) Discovery* started from Reykjavik, Iceland on 20th May 2022 and ended in Southampton on 26th June 2022. The ship first crossed the Atlantic Ocean to the east of Greenland before heading to the west coast and then sailing north. The *RRS* was stationed at four sites, Nuuk, Maniitsoq, Sisimut and the Davis Strait (near the melting sea ice). These four sites were selected together with the return leg over the Atlantic open ocean (18th-22nd June, named Wayback) considered as five locations to observe and analyze the formation of MSA at different latitudes. All the time in this study is in Universal Time Coordinated (UTC). The ship track and the five locations of the cruise are shown in Fig. 1.

During the cruise, all instruments were mounted in air-conditioned (18 °C) containers on the fore deck of the ship. A commercial $PM_{2.5}$ cyclone (at nominal flow rate of 16.7 LPM) was installed on the roof of one of the containers and operated at flow rate of 10 LPM to remove particles larger than PM_4. A HR-ToF-AMS with $PM_{2.5}$ lens and standard vaporizer was employed to measure the mass concentration of inorganic and organic aerosol and was operated using V-mode at a time resolution of 1 min. Particle number size distributions between 12.6 and 870 nm of the aerosol were measured concurrently by Scan Mobility Particle Sizer (SMPS, TSI Inc. USA, including DMA 3080, CPC 3776 at flow 0.3 LPM) with 5-minute resolution. Other species such as gaseous MSA (gMSA), DMS and Dimethyl sulfoxide (DMSO) was measured by Api-ToF-CIMS (Aerodyne Res, USA) and PTR-Qi-ToF-MS (IONICON, Austria). Ozone (O_3) was measured by a Thermo 49i ozone analyser (ThermoFisher Scientific, USA). Chlorophyll *a* (Chl-*a*) was derived from particulate absorption measured using a WETLabs AC-S (hyperspectral absorption-attenuation meter). Meteorological data were collected at a frequency of 10 Hz by Metek sonic anemometer (Metek, Germany).

HR-ToF-AMS calibrations were performed prior to the cruise in the laboratory, including lens alignment, vaporizer heater temperature, MCP voltage, Tof working voltages, flow rate, peak position and nitrate ionization efficiency (IE). A series of laboratory and in-field calibrations were also carried out for the relative IE (RIE) of nitrate, sulfate, ammonium and their peak position (Canagaratna et al., 2007; Hodshire et al., 2019; Zhang et al., 2018, 2022). A constant collection efficiency (CE) of 0.5 was used for the general chemical species (organics, sulfate, nitrate, ammonium and chloride). The RIE of nitrate, sulfate and ammonium was determined as 1.1, 0.96 and 4.69 respectively. A good correlation with R^2 of 0.91 was found between the sum of organics, sulfate, nitrate, ammonium and chloride (ΣOSNAC) and mass concentration derived from SMPS (Fig. S1 in supplement file). MSA calibrations were performed separately before, during and after the cruise. The methodology and calibration procedures for MSA are described in the next sections.

Ship emissions were most avoided during the whole cruise. When it was stationed, the ship was oriented towards the wind to avoid contamination. Even though, it is not possible to avoid ship plume contamination all the time, e.g., when the wind blew from the ship's stern, since there was no MSA in the ship exhaust, it is not necessary to filter the data. To further validate this, we compared the temporal variations of MSA with and without ship emission mask (Fig. S2 in supplement file). No obvious increase of MSA was observed during ship emission events, so we kept all data of MSA for this study.

2.2. Quantification of MSA

Quantification of MSA from HR-ToF-AMS is complicated because MSA fragments to several organic ions. In addition, ions such as SO^+ and SO_2^+ can also originate from inorganic aerosol sulfate species. Amongst these fragments, $CH_3SO_2^+$ has been reported as being highly specific ion of MSA in HR-ToF-AMS mass spectra by Phinney et al. (2006). The fraction of CH_3SO_2 (f (CH_3SO_2)) and relative ion efficiency of MSA (RIE_{MSA}) are two key parameters to determine MSA concentrations. In

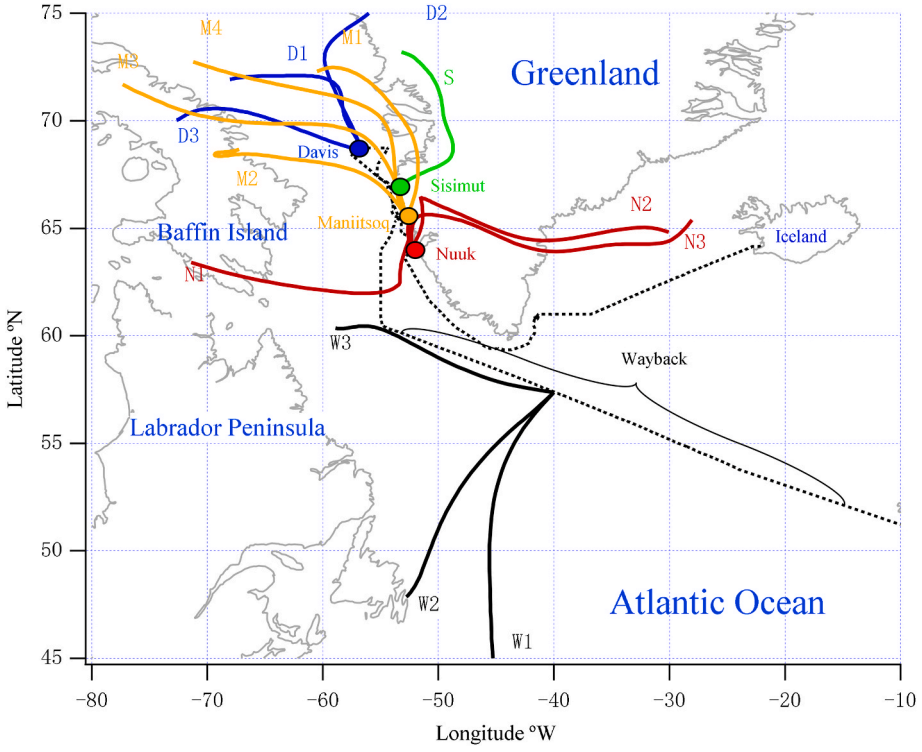

Fig. 1. The ship tracks, five locations (Davis Strait, Sisimut, Maniitsoq, Nuuk and Wayback) and their 72-h back trajectories cluster during the whole cruise. Ship tracks are in dash line, five locations are in colour dots, back trajectories are in colour solid lines (D1, D2 and D3 for Davis; S for Sisimut; M1, M2, M3 and M4 for Maniitsoq; N1, N2 and N3 for Nuuk; W1, W2 and W3 for Wayback).

this study, pure poly-dispersed MSA aerosol particles were used to obtain the mass spectra to determine f (CH_3SO_2), and a neutral solution of ammonium MSA (named AMSA) was used to determine the RIE_{MSA}. Finally, f (CH_3SO_2) of 3.1% and RIE_{MSA} of 1.61 were adopted for MSA quantification. The detailed quantification and calibration procedures are described in the Supplementary file text S2.

2.3. Quantification of nss-SO_4

Nss-SO_4 and sea-salt sulfate (ss-SO_4) can both contribute to the sulfate concentrations measured by an HR-ToF-AMS. The contribution of nss-SO_4 was evaluated by subtracting the ss-SO_4 concentration from the total sulfate concentration. The ss-SO_4 was estimated as 0.25 times the concentration of Na^+ (0.25 is the mass ratio of sulfate to Na^+ in the sea water) based on previous studies (Bates et al., 2001; Huang et al., 2017), whereas others employed 7.7% of total sea salt measured by HR-ToF-AMS (Ovadnevaite et al., 2012, 2014). In this study, we adopted 7.7% of total sea salt as ss-SO_4 to quantify nss-SO_4. Sea salt concentrations were quantified from HR-ToF-AMS measurements by independent laboratory and field calibrations (Fig. 2). The details for sea salt quantification are given in a companion paper (in preparation).

2.4. Clustering of the air mass back trajectories

Air mass back trajectories were calculated using Hybrid Single-Particle Lagrangian Integrated Trajectory, a transport and dispersion model developed by the NOAA Air Resources Laboratory (Stein et al., 2015). The hourly back trajectories at the four sites and one open Ocean point (Wayback) were calculated every hour for an arrival height of 100 m and length of 72 h respectively. The individual back trajectories were clustered using Euclid clustering distance algorithm. The cluster analysis yielded an optimal number of 3, 1, 4, 3 and 3 clusters for Davis Strait, Sisimut, Maniitsoq, Nuuk and Wayback, respectively. Four major air masses were classified which included air masses that had passed over sea ice, Greenland Island, Baffin Island and Atlantic open ocean.

3. Results

3.1. MSA and nss-SO_4

Time series of particulate MSA, nss-SO_4, Chlorophyll *a* (Chl *a*), DMS, sea salt and meteorological parameters for the whole cruise are shown in Fig. 2. Throughout the whole cruise, the average MSA concentration was 0.025 ± 0.03 μg m^{-3}, ranging from <0.01 to 0.32 μg m^{-3}. The highest MSA concentrations were observed over the Atlantic open ocean (53°40′ N and 23°50′ W) on the return leg. The lowest concentrations were observed near Sisimut (66°54′ N and 53°36’ W). The nss-SO_4 mass concentrations varied.

from <0.01 to 1.32 μg m^{-3}, with an average of 0.28 ± 0.24 μg m^{-3} during the cruise. The highest mean value of nss-SO_4 was observed at Nuuk, and the lowest at Davis Strait and Maniitsoq. The statistics of MSA and nss-SO_4 at five locations (Davis Strait, Sisimut, Maniitsoq, Nuuk, Wayback) were summarized in the box plot (Fig. 3 and Table S2). The median MSA concentration at the Davis Strait, Sisimut, Maniitsoq, Nuuk and Wayback was 0.01, 0.01, 0.014, 0.029, 0.032 μg m^{-3}, respectively. The median concentration of nss-SO_4 at the five locations was 0.09, 0.18, 0.14, 0.63, 0.34 μg m^{-3} respectively.

Latitude and temperature-based bin distribution of MSA/nss-SO_4 are displayed in Fig. 4a and b, respectively. The average value of MSA/nss-SO_4 was 0.1, ranging from 0.01 to 0.6, with most of the ratios fluctuating between 0.01 and 0.2 during the whole cruise. The correlation between

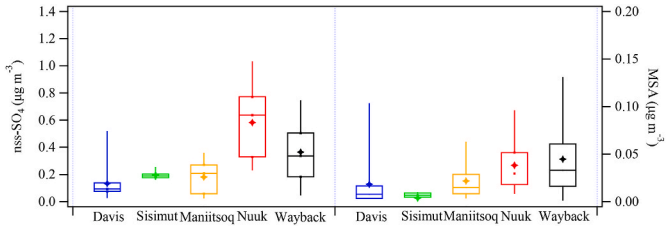

Fig. 3. Box plot (5%, 25%, median, 75%, 95% and mean) for nss-SO_4 and MSA at five locations. Mean values are in star, median and percentile values are in line.

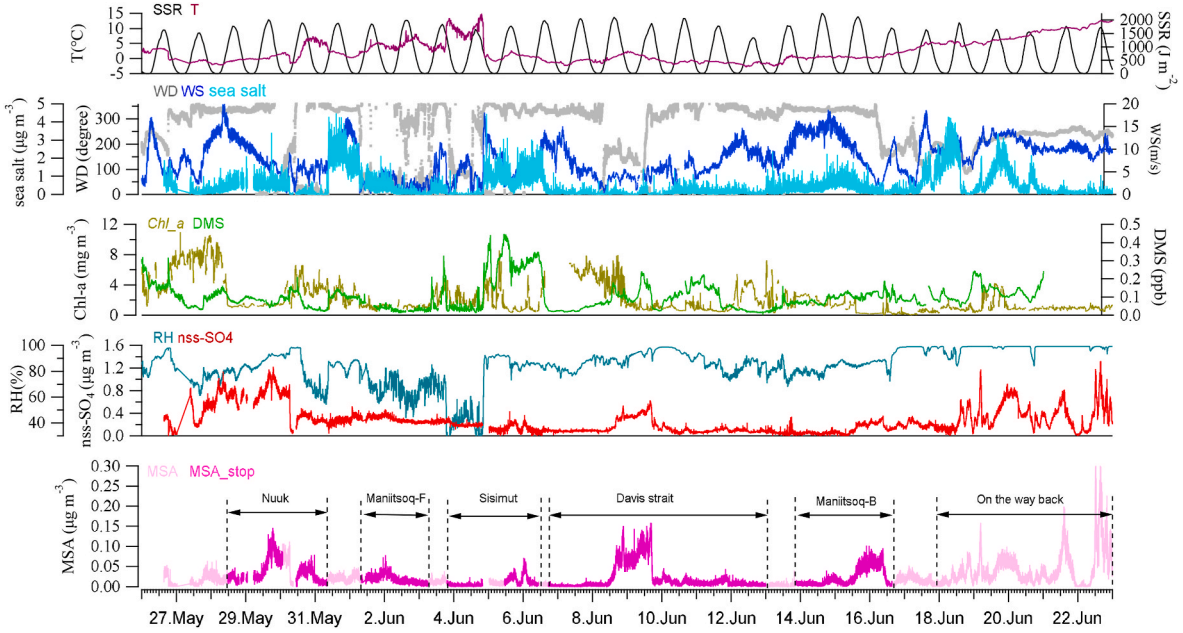

Fig. 2. Temporal variations of MSA, nss-SO_4, relative humidity (RH), Chl *a*, DMS, sea salt, wind speed (WS), wind direction (WD), surface solar radiation (SSR, downloaded from hourly ERA5 dataset), air temperature (T) and the ship locations during the cruise. The dark pink points in MSA represent the site measurements, and the ship positions are marked within the dash line respectively.

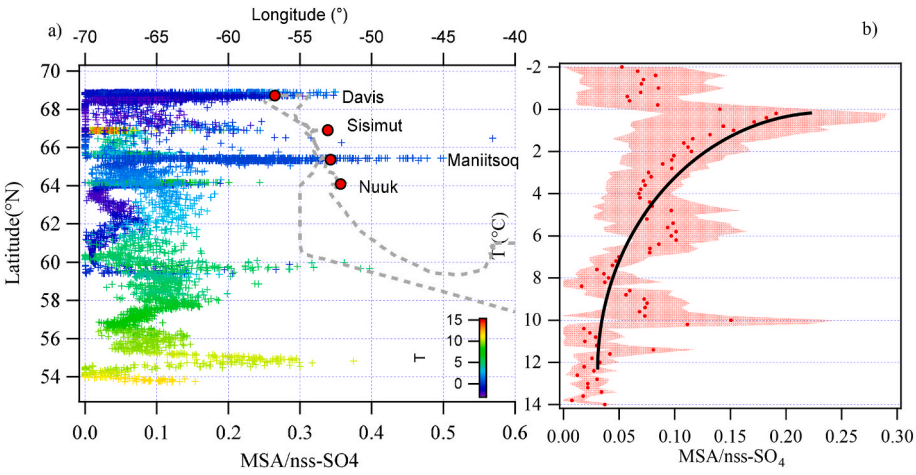

Fig. 4. Latitude (a) and air temperature bin distributions of MSA/nss-SO_4 (b) during the whole cruise. In Figure a, the dash line is the ship track, the red dots represent the sites where the ship was stationed.

MSA and nss-SO_4 for the whole cruise is presented in Fig. S8, and three groups with slopes of 0.23, 0.082 and 0.035 were identified.

3.2. Diurnal cycles of MSA and its related species

The diurnal cycles of gMSA, MSA, nss-SO_4, O_3, DMS, DMSO, sea salt, surface solar radiation (SSR), wind speed (WS) and relative humidity (RH) combined from four site measurements are displayed in Fig. 5. Similar diurnal cycles for DMS, DMSO, sea salt, WS and RH were found with two peaks around 11:00–13:00 and 22:00–24:00 (Fig. 5a and b). An obvious solar radiation peak around 15:00–18:00 was observed. O_3 exhibited a bimodal pattern with peaks in the early morning (7:00) and evening (20:00) (Fig. 5c), with an opposite trend to that of RH and solar radiation. gMSA, MSA and nss-SO_4 peaked during the late afternoon (17:00) which just following the peak of SSR and peaked in the evening (20:00), then slowly decreased through the night (Fig. 5c). The gMSA concentration appeared another earlier peak around 14:00 comparing with that of MSA and nss-SO_4. The evening peak of gMSA, MSA and nss-SO_4 matched well with the evening peak of O_3.

4. Discussions

4.1. MSA, nss-SO_4 and Chl-a levels over the North Atlantic and Arctic area

The median concentrations of particulate MSA observed in this study

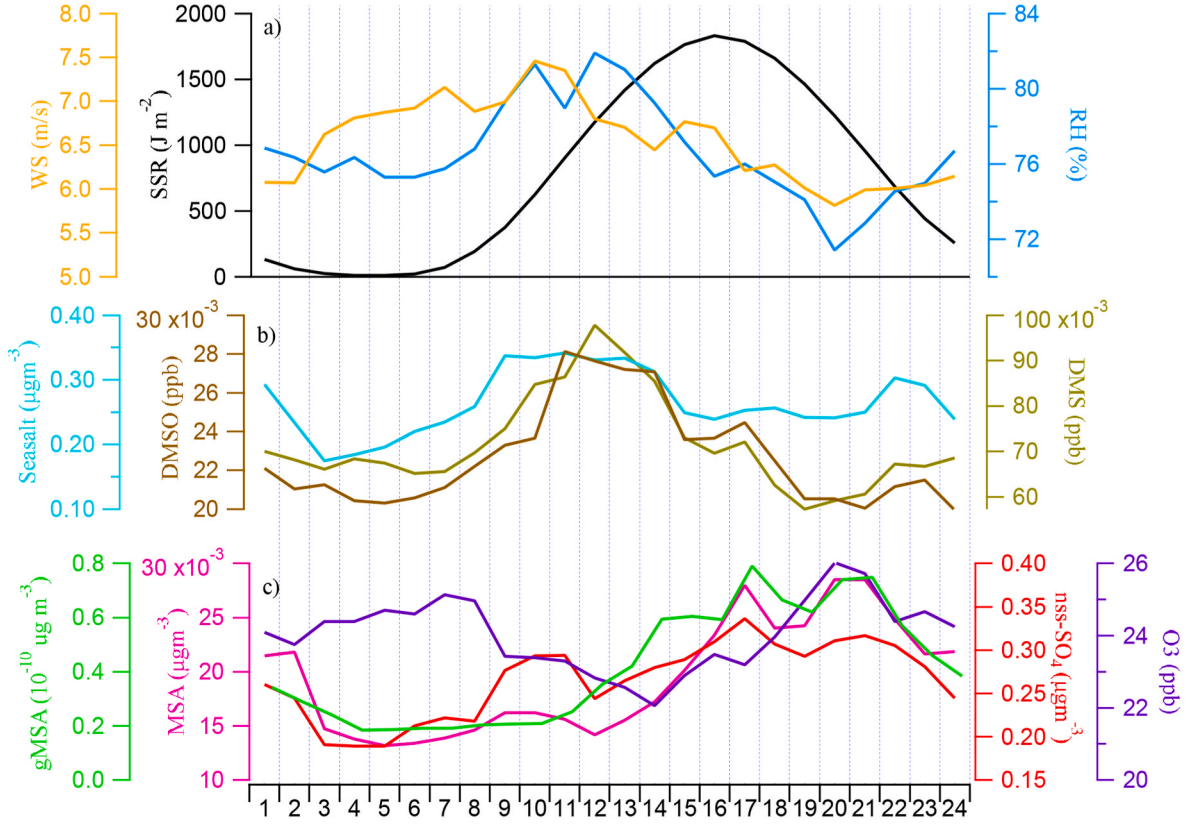

Fig. 5. Diurnal cycle of wind speed (WS), SSR, RH (a), sea salt, DMS, DMSO (b), gMSA, MSA, O_3, nss-SO_4 (c) combined from four stop measurements during the cruise.

varied from 0.01 to 0.032 μg m^{-3}, which is similar to those observed in summer over the Atlantic Ocean in its northern (0.02–0.04 μg m^{-3}), tropical (0.042 μg m^{-3}) and southern regions (from <0.01 to 0.04 μg m^{-3}). They were slightly lower than the median concentrations observed at Mace Head (0.05 μg m^{-3}) in summer (Ovadnevaite et al., 2014), Cape Verde Island off west Africa (14°55′ N, 23°31′ W) in summer (0.03 μg m^{-3}) (Müller et al., 2010) and the Bering Sea (52°47′-63°41′N, 161°43′-176°16′E) (0.038 μg m^{-3}) in July (Xu et al., 2005). Compared with previous measurements over the Northeast Pacific Ocean (average 0.16 ± 0.05 μg m^{-3}) during summer time (Phinney et al., 2006), our measured concentrations were significantly lower. These studies indicate that MSA concentrations over the Atlantic Ocean have remained stable within the last decade. Sharma et al. (2019) also reported no trend in long-term measurements of MSA from 1980 to 2013 at Alert, Canada (82°30′ N, 62°21′ W).

As a secondary product of DMS, MSA is directly linked to emissions from marine phytoplankton. Several studies have shown episodes of high MSA concentrations that correlate with blooms of DMS-producing phytoplankton along the California coast in an inland location of riverside (Gaston et al., 2010; Huang et al., 2015a). The concentrations of MSA might depend on both the origin of the sampled air mass and the concentration of oceanic Chl *a* (Gaston et al., 2010). Phinney et al. (2006) found good correlations between MSA concentration and oceanic biological activities over the northeast Pacific Ocean. Recent studies highlight strong gradients and variability in DMS tied to hydrographic features (e.g. sea ice melting, primary production of biogenic aerosol), specific phytoplankton groups or species speciation and biomass (Jarníková et al., 2018; Lizotte et al., 2020). However, no correlation between MSA and Chl *a* was found in this study. For instance, on 29th May at Nuuk area, a high MSA concentration (0.1 μg m^{-3}) was observed, while the Chl *a* concentration was low. Similarly, at the David strait, higher Chl *a* mass concentration (around 7 mg m^{-3}) was observed, but MSA concentration was very low. Over the open ocean (Atlantic), peak MSA concentration of 0.20 and 0.29 μg m^{-3} were observed on 22nd and 23rd June, respectively, whereas corresponding Chl *a* levels were very low. Several previous studies also found no relationship between MSA and Chl-*a* (Becagli et al., 2013; Huang et al., 2017; Jung et al., 2014). The reason for the low correlation between MSA and Chl *a* may be that only certain phytoplankton groups (Prymnesiophytes and Dinoflagellates) produce DMS. It was reported that the presence of strong DMS producers, especially the haptophyte Phaeocystis, drives high DMS concentrations in the Arctic Ocean (Galí et al., 2021). And Chl *a* represents the biomass of the entire phytoplankton community rather than these specific groups. Furthermore, DMS can also be produced by bacteria and zooplankton mediated grazing (Dacey and Wakeham, 1986; Gabric et al., 2001) which are not reflected by the Chl *a* level. The release of DMS, which is produced by ice algae and phytoplankton trapped under the ice or in melt ponds during sea ice retreat or melt, can contribute to high MSA concentrations in the sea-ice covered areas (Galindo et al., 2014). As reviewed by Stefels et al. (2007), there is no direct relationship between DMS and Chl *a* on a global scale, since the precursor of DMS is produced by diverse phytoplankton at different rates, which vary with physiological state. On the other hand, the measured MSA could be impacted by many factors. Different pathways of DMS oxidation should be considered, including gas-phase, heterogeneous, and aqueous reactions, the regional transported particles, and removal of MSA by dry and wet deposition (Huang et al., 2017) also make the relationship more complex. Use Chl *a* as a biological surrogate for marine organic particles is still under debate (Bates et al., 2012; Huang et al., 2017; Quinn et al., 2014). Caution should be taken when using Chl *a* as an indicator of marine DMS generation.

4.2. Evolution of MSA and the oxidation path from DMS

DMS in the ocean is released to the atmosphere at the ocean surface with its gas transfer coefficients demonstrably rising alongside with wind speed, and consequently, the intensity of breaking waves (Blomquist et al., 2017). Similar diurnal cycles for sea salt, WS, and DMS (Fig. 5) appear to reflect the link between wave breaking and primary emission of DMS into the marine atmosphere.

For the secondary product, DMSO first reached peak concentration during 11:00–14:00 with the solar radiation increasing, and then began to decline when the gMSA, MSA and nss-SO_4 increased. The variation of DMSO suggests that it is a very important precursor for MSA and/or sulfate formation. Previous oxidation experiments have shown the reaction of DMSO with OH could yield two major sulfur-containing products, i.e. MSA and H_2SO_4 (Hoffmann et al., 2016; Ning and Zhang, 2022; Shen et al., 2022). Zhang et al. (2014) suggested the precursor of a strong daytime source of MSA may be DMSO. Additionally, Jiang et al. (2021, 2022) also observed MSA formation by DMSO initiated by photo-oxidation in laboratory work. All these studies point out the importance of DMSO pathway in MSA formation process.

Model studies suggested that the photo-oxidation by OH (60–84%) (Chen et al., 2018; Hoffmann et al., 2016), BrO (46%) (Hoffmann et al., 2016) and NO_3 (16%) radicals are the main oxidation pathways for DMS to produce DMSO, MSA and its intermediates (CH_3SO_2H, MSIA) (Hoffmann et al., 2016; Ning and Zhang, 2022; Veresa et al., 2020). Solar radiation, RH and O_3 are three key factors for primary OH production (Seinfeld and Pandis, 2012). The O_3 diurnal cycle shows lower concentration during daytime and higher at night (Fig. 5c). The O_3 loss pattern during the day might both by the photolysis and physical boundary layer variation, and the recovery at night may be due to the O_3 entrainment from the free troposphere (Read et al., 2008) and lower boundary layer mixing height. As solar radiation and RH increased, the existing O_3 would experience short-wavelength photolysis reaction and generate OH radicals. Other model studies also reported that halogen chemistry (IO and BrO) has a significant influence on photochemical O_3 and OH (Glasow et al., 2004; Read et al., 2008; Yang et al., 2005), and BrO would cause marked changes in DMS levels and oxidation pathways (Glasow et al., 2004). In terms of higher concentrations of MSA (both in gas and particulate phase), nss-SO_4 at 21:00–22:00, as the weak photochemical activity, lower boundary layer mixing height (Fig. S7) might be the key factor.

4.3. Temperature dependence of MSA/nss-SO_4

The latitude distribution of MSA/nss-SO_4 ratios (Fig. 4a) shows that higher MSA/nss-SO_4 values (0.2–0.6) occurred at Davis, Maniitsoq and on the cruise return leg (near 60 °N and 55 °N). These values are larger than previous observations made over the Atlantic Ocean in summer time, such as at Mace Head (0.11–0.13) (Ovadnevaite et al., 2014) (temperature 11–18 °C), Barbados (0.055) (Savoie et al., 2002) (temperature 23–30 °C), tropical Atlantic (0.02) (van Pinxteren et al., 2015) (temperature above 30 °C) and southern Atlantic (0.14) (Lin et al., 2012) (temperature above 20 °C). Globally, the ratio of MSA to nss-SO_4 varied from about 0.1 near the equator to nearly 0.4 in Atlantic waters (Seinfeld and Pandis, 2012), and the value varied from 0.05 to 0.75, usually below 0.5 at seven different meteorological/oceanographic regimes in Northern and Southern Hemisphere (Bates et al., 2001; Shen et al., 2022).

An inverse relationship between MSA/nss-SO_4 ratio and temperature was found, the ratio decreased from 0.2 to 0.03 while the temperature increased from 0 °C to 14 °C (Fig. 4a). This phenomenon indicates temperature may be a factor influencing the ratio. The colder the temperature, the more MSA was formed, as opposed to SO_2 and eventually to sulfuric acid. This behavior was consistent with the competition between a radical decomposition step with large activation energy and a bimolecular reaction with small activation energy (Seinfeld and Pandis, 2012). Modelling studies also suggested that decreasing the temperature enhances the gas-phase MSA production by an order of magnitude from OH-initiated DMS oxidation (Shen et al., 2022). Under warmer conditions, thermal decay of CH_3SO_3 represented the main contributor to sulfuric acid (Hoffmann et al., 2016; Shen et al., 2022).

The ratios of MSA to nss-SO_4 under subzero temperature condition (<0 °C) did not follow the temperature dependence rule but exhibited stable values around 0.04–0.08. One reason might be the release of DMS from the ocean surface under the low temperature was not as active as at higher temperature, causing low MSA production. The other one is that hydrogen abstraction by OH and via isomerization (autoxidation) was suppressed at a lower temperature (Shen et al., 2022). The behaviour of DMS oxidation under subzero temperature conditions are still challenging to be investigated experimentally, which needs more attention in the future.

The inverse relationship between MSA/nss-SO_4 and temperature was also reported by Bates et al. (2001) over the Pacific Ocean, between 20 °N and 60 °S and from the ice core records at Renland in Greenland (Hansson and Saltzman, 1993). Moreover, the Cosmics Leaving Outdoor Droplets (CLOUD) chamber experiment at CERN also confirmed that the ratio of H_2SO_4/MSA was mainly determined by temperature instead of precursor vapor concentrations (Shen et al., 2022), which also supports this conclusion.

4.4. *Determining a reference value of MSA/nss-SO_4 for the remote marine atmosphere*

The ratio of MSA to nss-SO_4 is often used to assess the natural and anthropogenic contributions to sulfate. This differentiation is important, as nss-SO_4 could origin from both DMS oxidation (Gros et al., 2022; Schmale et al., 2021) and other sources such as volcanoes, long-range transport, and anthropogenic activities (Huang et al., 2017; Ovadnevaite et al., 2014). On the other hand, air masses with different oxidation histories may lead to different conversion efficiencies of DMS to MSA, thus resulting in different MSA/nss-SO_4 ratios. It is useful to determine the reference value of MSA/nss-SO_4 derived from remote marine atmosphere. In this study, we investigated the relationship between MSA and nss-SO_4 as well as air mass cluster analysis across five locations to identify a reference MSA/nss-SO_4 ratio that accurately represents the remote marine atmospheric conditions.

Fig. 6 displays the correlation between MSA and nss-SO_4 and their air mass back trajectories at all five locations. According to the linear curve fitting correlation slopes, three groups with higher (in green), moderate (in blue) and low ratios of MSA to nss-SO_4 (in red) were classified. At Davis Strait, only one group was observed, with a slope of 0.25 and a correlation coefficient (R^2) of 0.91. Two groups with slope of 0.25 (R^2 = 0.83) and 0.15 (R^2 = 0.57) at Maniitsoq represent the measurements headed north and south respectively. Two groups (slope = 0.22, R^2 = 0.93; slope = 0.1, R^2 = 0.67) and three groups (slope = 0.03, R^2 = 0.42; slope = 0.11, R^2 = 0.48; slope = 0.19, R^2 = 0.54) were observed at Wayback and Nuuk respectively. Good correlations between MSA and nss-SO_4 at Davis Strait, Maniitsoq, Nuuk and Wayback were found, while the correlation between MSA and nss-SO_4 at Sisimut was weak (R^2 = 0.19).

Back trajectory cluster analysis indicates Davis Strait and Maniitsoq were significantly influenced by air masses that passed over sea ice from the northern polar region. Those points with high and moderate ratio at Nuuk and Wayback were mainly affected by air masses from the open Atlantic Ocean. However, the low ratios at Sisimut and Nuuk were dominantly influenced by air mass from Greenland Island and Baffin Island respectively. Given the absence of anthropogenic activities in the northern polar region and the open Ocean, the groups influenced by these air masses should be considered as representative of the clean marine atmosphere. Among these groups, only higher ratio groups at Davis Strait (0.25), Mannitsoq (0.25) and Wayback (0.22) cross the origin point, indicating the fresh MSA and nss-SO_4 formation process. Therefore, a ratio range of 0.22–0.25 is recommended to more accurately reflect the natural behaviour of DMS oxidation into MSA and nss-SO_4, and they are considered as the reference MSA/nss-SO_4 ratio of remote marine atmosphere. This reference ratio is higher than the 0.1 reported at Mace Head (Ovadnevaite et al., 2014) and 0.149 during Atlantic clean events, while is consistent with the 0.26 reported in Megacity Paris by separating nss-SO_4 of marine origin from that of anthropogenic origin (Crippa et al., 2013). Even though the ratio of MSA to nss-SO_4 can be used to assess the natural and anthropogenic sulfate contribution, as it might be influenced by multiple factors, the limitations of this method need to be concerned.

For other groups, minimum nss-SO_4 concentrations about 0.2–0.6 μg m^{-3} and lower ratios were observed. The offset concentration of sulfate would due to anthropogenic sulfate being introduced by regional transportation, e.g. Nuuk mainly dominated by air masses passing over

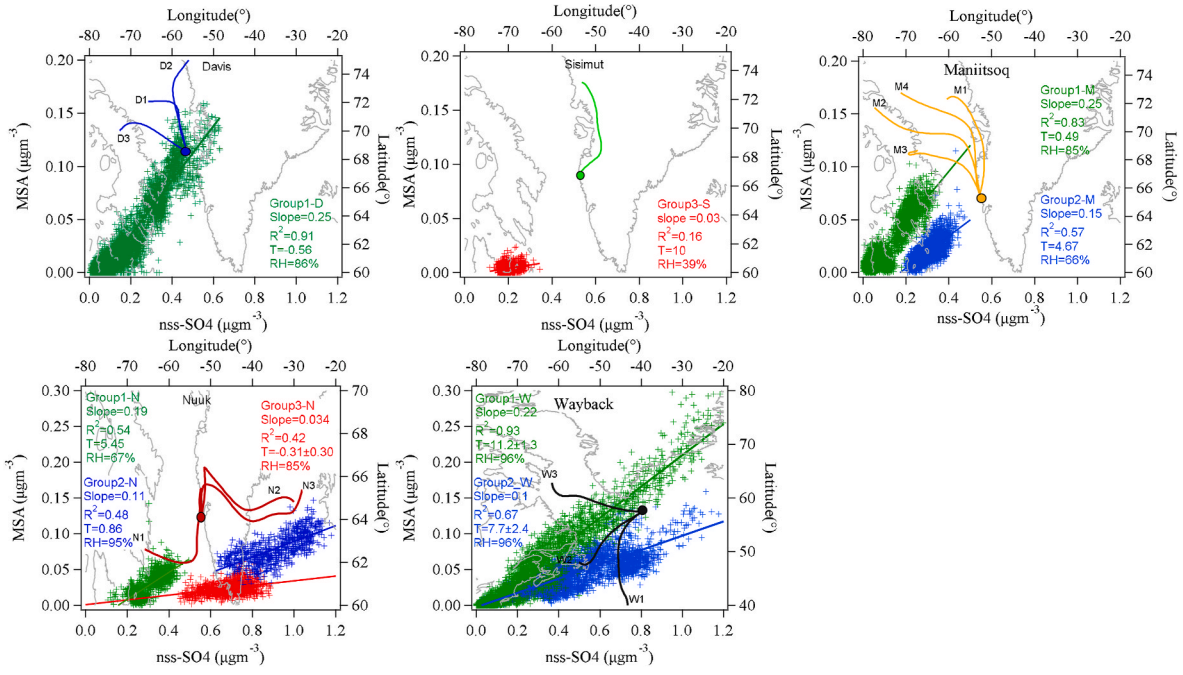

Fig. 6. Correlation plots between MSA and nss-SO_4 at the five locations. Different groups for high, moderate and low slopes are displayed in green, blue and red markers, respectively. The coloured solid lines in each plot represent the back trajectory of air mass.

the less remote Baffin Island (Schmale et al., 2021) and the accumulations of preexist sulfate. The lower ratios would be impacted by multiple factors, including anthropogenic sulfate contributions, different oxidation histories of marine origin air masses, removal (or deposition) of MSA and sulfate, and complex processes for of MSA and nss-SO_4 formation which need further model studies to verify in the future.

5. Conclusion

The mass concentration of methane sulfonic acid (MSA) and non-sea salt sulfate (nss-SO_4) were quantified using a method validated through measurements from a high resolution time-of-flight Aerosol Mass Spectrometer (HR-ToF-AMS), highlighting their significance in understanding DMS oxidation into MSA and nss-SO_4. We found average concentrations of MSA and nss-SO_4 were 0.025 ± 0.030 μg m^{-3} and 0.28 ± 0.24 μg m^{-3} during the cruise respectively, with MSA lower in the northern leg and nss-SO_4 higher over open Ocean. The observed diurnal patterns of MSA, nss-SO_4 and their related species underline the importance of photochemical process in DMS oxidation. An inverse relationship between MSA/nss-SO_4 and air temperature indicated low temperatures favored MSA formation. MSA/nss-SO_4 ratios of 0.22–0.25 are suggested as reference values of remote marine atmosphere. Our findings support the dominant role of photochemistry in the formation of MSA and nss-SO_4 from DMS, recommending further investigation into thermal decay pathways for sulfate formation and the complex DMS oxidation mechanism.

CRediT authorship contribution statement

Yangmei Zhang: Writing – original draft, Methodology, Formal analysis, Data curation, Conceptualization. **Junying Sun:** Supervision, Conceptualization. **Xiaojing Shen:** Data curation. **Vipul Lal Chandani:** Investigation, Formal analysis. **Mao Du:** Methodology, Data curation. **Congbo Song:** Validation, Project administration, Data curation. **Yuqing Dai:** Software. **Guoyuan Hu:** Software. **Mingxi Yang:** Methodology, Formal analysis, Data curation. **Gavin H. Tilstone:** Software, Formal analysis, Conceptualization. **Tom Jordan:** Resources, Data curation. **Giorgio Dall'Olmo:** Software. **Quan Liu:** Software. **Eiko Nemitz:** Supervision, Methodology. **Anna Callaghan:** Data curation. **James Brean:** Resources, Data curation. **Roberto Sommariva:** Data curation. **David Beddows:** Investigation. **Ben Langford:** Methodology. **William Bloss:** Resources. **William Acton:** Data curation. **Zongbo Shi:** Writing – review & editing, Supervision, Project administration, Funding acquisition, Conceptualization.

Declaration of competing interest

The authors declare the following financial interests/personal relationships which may be considered as potential competing interests: Yangmei Zhang reports financial support was provided by National Natural Science Foundation of China. Yangmei Zhang reports financial support was provided by Chinese Academy of Meteorological Sciences. Zongbo Shi reports financial support was provided by Natural Environment Research Council. If there are other authors, they declare that they have no known competing financial interests or personal relationships that could have appeared to influence the work reported in this paper.

Data availability

Data will be made available on request.

Acknowledgement

This work was funded by the National Natural Science Foundation of China (Grant No. 42175128), Sci & Tech Development Foundation of CAMS (Grant No. 2022KJ005, 2022KJ002), Basic Research Fund of CAMS (2023Z012). DY151 cruise is funded by UK Natural Environment Research Council under the following grants: NE/S00579X/1 (PI Zongbo Shi), NE/S005587/1 (PI Anna Jones), and NE/T00648X/1 (PI Ben Murray). GHT, TJ and GD'O were funded by AMT4CO2Flux (contract number 4000136286/21/NL/FF/ab) from the European Space Agency. We wish to thank the captain Antione Gatti and the crew of the RRS Discovery, and the National Marine Facility (NMF) team, including NMF technicians (Jon Short, Jack Arnott and Nick Harker) for their support before, during and after the DY151 cruise. We thank the technical supports from Leah William, Philip Croteau and Bill Brooks for the MSA calibration method instruction, AMS measurements and timely troubleshooting. We also thank all the scientist team for their support, discussions and cooperation throughout the campaign.

Appendix A. Supplementary data

Supplementary data to this article can be found online at https://doi.org/10.1016/j.atmosenv.2024.120538.

References

Bates, T.S., Quinn, P.K., Coffman, D.J., Johnson, J.E., Miller, T.L., Covert, D.S., Wiedensohler, A., Leinert, S., Nowak, A., Neusüss, C., 2001. Regional physical and chemical properties of the marine boundary layer aerosol across the Atlantic during Aerosols99: an overview. J. Geophys. Res. Atmos. 106 (D18), 20767–20782.

Bates, T.S., Quinn, P.K., Frossard, A.A., Russell, L.M., Hakala, J., Petäjä, T., Kulmala, M., Covert, D.S., Cappa, C.D., Li, S.-M., Hayden, K.L., Nuaaman, I., McLaren, R., Massoli, P., Canagaratna, M.R., Onasch, T.B., Sueper, D., Worsnop, D.R., Keene, W. C., 2012. Measurements of ocean derived aerosol off the coast of California. J. Geophys. Res. 117, D00V15.

Becagli, S., Amore, A., Caiazzo, L., Iorio, T.D., Sarra, A.d., Lazzara, L., Marchese, C., Meloni, D., Mori, G., Muscari, G., Nuccio, C., Pace, G., Severi, M., Traversi, R., 2019. Biogenic aerosol in the arctic from eight years of MSA data from ny Ålesund (Svalbard Islands) and Thule (Greenland). Atmosphere 10 (349), 1–12.

Becagli, S., Lazzara, L., Fani, F., Marchese, C., Traversi, R., Severi, M., di Sarra, A., Sferlazzo, D., Piacentino, S., Bommarito, C., Dayan, U., Udisti, R., 2013. Relationship between methanesulfonate (MS) in atmospheric particulate and remotely sensed phytoplankton activity in oligo-mesotrophic central Mediterranean Sea. Atmos. Environ. 79, 681–688.

Blomquist, B.W., Brumer, S.E., Fairall, C.W., Huebert, B.J., Zappa, C.J., Brooks, I.M., Yang, M., Bariteau, L., Prytherch, J., Hare, J.E., Czerski, H., Matei, A., Pascal, R.W., 2017. Wind speed and sea state dependencies of air-sea gas transfer: results from the high wind speed gas exchange study (HiWinGS). J. Geophys. Res.: Oceans 122, 8034–8062.

Bork, N., Elm, J., Olenius, T., Vehkamäki, H., 2014. Methane sulfonic acid-enhanced formation of molecular clusters of sulfuric acid and dimethyl amine. Atmos. Chem. Phys. 14, 12023–12030.

Canagaratna, M.R., Jayne, J.T., Jimenez, J.L., Allan, J.D., Alfarra, M.R., Zhang, Q., Onasch, T.B., Drewnick, F., Coe, H., Middlebrook, A., 2007. Chemical and microphysical characterization of ambient aerosols with the aerodyne aerosol mass spectrometer. Mass Spectrom. Rev. 26, 185–222.

Charlson, R.J., LovelockI, J.E., Andreaei, M.O., Warren, S., 1987. Oceanic phytoplankton, atmospheric sulphur, cloud. Nature 3526, 16.

Chen, Q., Sherwen, T., Evans, M., Alexander, B., 2018. DMS oxidation and sulfur aerosol formation in the marine troposphere: a focus on reactive halogen and multiphase chemistry. Atmos. Chem. Phys. 18, 13617–13637.

Chen, Y., Xu, L., Humphry, T., Hettiyadura, A.P.S., Ovadnevaite, J., Huang, S., Poulain, L., Schroder, J.C., Campuzano-Jost, P., Jimenez, J.L., Herrmann, H., O'Dowd, C., Stone, E.A., Ng, N.L., 2019. Response of the aerodyne aerosol mass spectrometer to inorganic sulfates and organosulfur compounds: applications in field and laboratory measurements. Environ. Sci. Technol. 53, 5176–5186.

Crippa, M., Haddad, I.E., Slowik, J.G., DeCarlo, P.F., Mohr, C., Heringa, M.F., Chirico, R., Marchand, N., Sciare, J., Baltensperger, U., Prévôt, A.S.H., 2013. Identification of marine and continental aerosol sources in Paris using high resolution aerosol mass spectrometry. J. Geophys. Res. Atmos. 118, 1950–1963.

Dacey, J.W.H., Wakeham, S.G., 1986. Oceanic dimethylsulfide: production during zooplankton grazing on phytoplankton. Science 233 (4770), 1314–1316.

Dall'Osto, M., Simo, R., Harrison, R.M., Beddows, D.C.S., Saiz-Lopez, A., Lange, R., Skov, H., Nøjgaard, J.K., Nielsen, I.E., Massling, A., 2018. Abiotic and biotic sources influencing spring new particle formation in North East Greenland. Atmos. Environ. Times 190, 126–134.

Gabric, A.J., Whetton, P.H., Cropp, R., 2001. Dimethylsulphide production in the subantarctic southern ocean under enhanced greenhouse conditions. Tellus, Ser. B 53 (3). ISSN 0013− 0936X.

Galí, M., Lizotte, M., Kieber, D.J., Randelhoff, A., Hussherr, R., Xue, L., Dinasquet, J., Babin, M., Rehm, E., Levasseur, M., 2021. DMS emissions from the Arctic marginal ice zone. Elem. Sci. Anthr. 9, 00113.

Galindo, V., Levasseur, M., Mundy, C.J., Gosselin, M., Tremblay, J.-E., Scarratt, M., Gratton, Y., Papakiriakou, T., Poulin, M., Lizotte, M., 2014. Biological andphysical processes influencing sea ice,under-ice algae, and dimethylsulfoniopropionate duringspring in the Canadian ArcticArchipelago. J. Geophys. Res. Oceans 119, 3746–3766. https://doi.org/10.1002/2013JC009497.

Gaston, C.J., Pratt, K.A., Qin, X.Y., Prather, K.A., 2010. Real-time detection and mixing state of methanesulfonate in single particles at an inland urban location during a phytoplankton bloom. Environ. Sci. Technol. 44 (5), 1566–1572.

Glasow, R.v., Kuhlmann, R.v., Lawrence, M.G., Platt, U., Crutzen, P.J., 2004. Impact of reactive bromine chemistry in the troposphere. Atmos. Chem. Phys. 4, 2481–2497.

Gros, V., Bonsang, B., Sarda-Estève, R., Nikolopoulos, A., Metfies, K., Wietz, M., Peeken, I., 2022. Variability of dimethyl sulphide (DMS), methanethiol and other trace gases in context of microbial communities from the temperate Atlantic to the Arctic Ocean. Biogeosci. Discuss. 1–25.

Hansson, M.E., Saltzman, E.S., 1993. The first Greenland ice core record of methanesulfonate and sulfate over a full glacial cycle. Geophys. Res. Lett. 20 (12), 1163–1166.

Hodshire, A.L., Campuzano-Jost, P., Kodros, J.K., Croft, B., Nault, B.A., Schroder, J.C., Jimenez, J.L., Pierce, J.R., 2019. The potential role of methanesulfonic acid (MSA) in aerosol formation and growth and the associated radiative forcings. Atmos. Chem. Phys. 19, 3137–3160.

Hoffmann, E.H., Tilgner, A., Schrödner, R., Bräuer, P., Wolke, R., Herrmann, H., 2016. An advanced modeling study on the impacts and atmospheric implications of multiphase dimethyl sulfide chemistry. Proc. Natl. Acad. Sci. USA 113 (42), 11776–11781.

Huang, D., Li, Y., Lee, B.P., Chan, C.K., 2015a. Analysis of organic sulfur compounds in atmospheric aerosols at the HKUST supersite in Hong Kong using HR-ToF-AMS. Environ. Sci. Technol. 49, 3672–3679.

Huang, D., Li, Y., Lee, B.P., Chan, C.K., 2015b. Analysis of organic sulfur compounds in atmospheric aerosols at the HKUST supersite in Hong Kong using HR-ToF-AMS. Environ. Sci. Technol. 49, 3672–3679.

Huang, S., Poulain, L., Pinxteren, D.v., Pinxteren, M.v., Wu, Z., Herrmann, H., Wiedensohler, A., 2017. Latitudinal and seasonal distribution of particulate MSA over the atlantic using a validated quantification method with HR-ToF-AMS. Environ. Sci. Technol. 51, 418–426.

Huang, S., Wu, Z., Poulain, L., Pinxteren, M.v., Merkel, M., Assmann, D., Herrmann, H., Wiedensohler, A., 2018. Source apportionment of the organic aerosol over the Atlantic Ocean from 53◦ N to 53◦ S: significant contributions from marine emissions and long-range transport. Atmos. Chem. Phys. 18, 18043–18062.

Jarníková, T., Dacey, J., Lizotte, M., Levasseur, M., Tortell, P., 2018. The distribution of methylated sulfur compounds, DMS and DMSP, in Canadian subarctic and Arctic marine waters during summer 2015. Biogeosciences 15, 2449–2465.

Jiang, H., Carena, L., He, Y., Wang, Y., Zhou, W., Yang, L., Luan, T., Li, X., Brigante, M., Vione, D., Gligorovski, S., 2021. Photosensitized degradation of DMSO initiated by PAHs at the air-water interface, as an alternative source of organic sulfur compounds to the atmosphere. J. Geophys. Res. Atmos. 126, 1–15 e2021JD035346.

Jiang, H., He, Y., Wang, Y., Li, S., Jiang, B., Carena, L., Li, X., Yang, L., Luan, T., Vione, D., Gligorovski, S., 2022. Formation of organic sulfur compounds through SO2-initiated photochemistry of PAHs and dimethylsulfoxide at the air-water interface. Atmos. Chem. Phys. 22, 4237–4252.

Jung, J., Furutani, H., Uematsu, M., Park, J., 2014. Distributions of atmospheric non-sea-salt sulfate and methanesulfonic acid over the Pacific Ocean between 48°N and 55°S during summer. Atmos. Environ. 99, 374–384.

Lin, C.T., Baker, A.R., Jickells, T.D., Kelly, S., Lesworth, T., 2012. An assessment of the significance of sulphate sources over the Atlantic Ocean based on sulphur isotope data. Atmos. Environ. 62, 615–621.

Lizotte, M., Levasseur, M., Galindo, V., Gourdal, M., Gosselin, M., Tremblay, J.-É., Blais, M., Charette, J., Hussherr, R., 2020. Phytoplankton and dimethylsulfide dynamics at two contrasting Arctic ice edges. Biogeosciences 17, 1557–1581.

Ma, H., Sun, B., Hu, Z., Shi, G., 2021. Studies on polar non-sea-salt sulfate (nssSO2– 4) and methanesulfonate (MSA) and their environmental indications Chinese. J. Polar Res. 33 (2), 171–182.

McGrath, M.J., Olenius, T., Ortega, I.K., Loukonen, V., Paasonen, P., Kurtén, T., Kulmala, M., Vehkamäki, H., 2012. Atmospheric Cluster Dynamics Code: a flexible method for solution of the birth-death equations. Atmos. Chem. Phys. 12, 2345–2355.

Müller, K., Lehmann, S., Pinxteren, D.v., Gnauk, T., Niedermeier, N., Wiedensohler, A., Herrmann, H., 2010. Particle characterization at the Cape Verde atmospheric observatory during the 2007 RHaMBLe intensive. Atmos. Chem. Phys. 10, 2709–2721.

Ning, A., Zhang, X., 2022. The synergistic effects of methanesulfonic acid (MSA) and methanesulfinic acid (MSIA) on marine new particle formation. Atmos. Environ. 269, 118826.

O'Dowd, C., Deleeuw, G., 2007. Marine aerosol production: a review of the current knowledge. Phil. Trans. R. Soc. A. 365, 1753–1774.

Olenius, T., Kupiainen-Määttä, O., Ortega, I., Kurtén, T., Vehkamäki, H., 2013. Free energy barrier in the growth of sulfuric acid–ammonia and sulfuric acid–dimethylamine clusters. J. Chem. Phys. 139, 084312.

Ovadnevaite, J., Ceburnis, D., Canagaratna, M., Berresheim, H., Bialek, J., Martucci, G., Worsnop, D.R., O'Dowd, C., 2012. On the effect of wind speed on submicron sea salt mass concentrations and source fluxes. J. Geophys. Res. 117, D16201.

Ovadnevaite, J., Ceburnis, D., Leinert, S., Dall'Osto, M., Canagaratna, M., O'Doherty, S., Berresheim, H., O'Dowd, C., 2014. Submicron NE Atlantic marine aerosol chemical composition and abundance: seasonal trends and air mass categorization. J. Geophys. Res. Atmos. 119, 11850–11863.

Phinney, L., Leaitch, W.R., Lohmann, U., Boudries, H., Worsnop, D.R., Jayne, J.T., Toom-Sauntry, D., Wadleigh, M., Sharma, S., Shantz, N., 2006. Characterization of the aerosol over the subarctic north east Pacific Ocean. Deep-Sea Res. II. 53, 2410–2433.

Quinn, P.K., Bates, T.S., Coffman, D.J., Covert, D.S., 2008. Influence of particle size and chemistry on the cloud nucleating properties of aerosols. Atmos. Chem. Phys. 8, 1029–1042.

Quinn, P.K., Bates, T.S., Schulz, K.S., Coffman, D.J., Frossard, A.A., Russell, L.M., Keene, W.C., Kieber, D.J., 2014. Contribution of sea surface carbon pool to organic matter enrichment in sea spray aerosol. Nat. Geosci. 7, 228–232.

Read, K.A., Mahajan, A.S., Carpenter, L.J., Evans, M.J., Faria, B.V.E., Heard, D.E., Hopkins, J.R., Lee, J.D., Moller, S.J., Lewis, A.C., Mendes, L., McQuaid, J.B., Oetjen, H., Saiz-Lopez, A., Pilling, M.J., Plane, J.M.C., 2008. Extensive halogen-mediated ozone destruction over the tropical Atlantic Ocean. Nature 453, 1232–1235.

Savoie, D.L., Arimoto, R., Keene, W.C., Prospero, J.M., Duce, R.A., Galloway, J.N., 2002. Marine biogenic and anthropogenic contributions to non-sea-salt sulfate in the marine boundary layer over the North Atlantic Ocean. J. Geophys. Res. 107 (D18), 4356.

Schmale, J., Zieger, P., Ekman, A.M.L., 2021. Aerosols in current and future Arctic climate. Nat. Clim. Change 11, 95–105.

Seinfeld, J.H., Pandis, S.N., 2012. Atmospheric Chemistry and Physics: from Air Pollution to Climate Change. John Wiley & Sons.

Sharma, S., Barrie, L.A., Magnusson, E., Brattström, G., Leaitch, W.R., Steffen, A., Landsberger, S., 2019. Afactor and trends analysis ofmultidecadal lower troposphericobservations of arctic aerosolcomposition, black carbon, ozone, andmercury at alert, Canada. Journal of Geophysical Research: Atmospheres 124 (14). https://doi.org/10.1029/2019JD030844, 133–14,161. https://doi.org/10.1029/2019JD030844.

Shen, J., Scholz, W., He, X.-C., Zhou, P., Marie, G., Wang, M., Marten, R., Surdu, M., Rörup, B., Baalbaki, R., Amorim, A., Ataei, F., Bell, D.M., Bertozzi, B., Brasseur, Z., Caudillo, L., Chen, D., Chu, B., Dada, L., Duplissy, J., Finkenzeller, H., Granzin, M., Guida, R., Heinritzi, M., Hofbauer, V., Iyer, S., Kemppainen, D., Kong, W., Krechmer, J.E., Kürten, A., Lamkaddam, H., Lee, C.P., Lopez, B., Mahfouz, N.G.A., Manninen, H.E., Massabò, D., Mauldin, R.L., Mentler, B., Müller, T., Pfeifer, J., Philippov, M., Piedehierro, A.A., Roldin, P., Schobesberger, S., Simon, M., Stolzenburg, D., Tham, Y.J., Tomé, A., Umo, N.S., Wang, D., Wang, Y., Weber, S.K., Welti, A., Jonge, R.W.d., Wu, Y., Zauner-Wieczorek, M., Zust, F., Baltensperger, U., Curtius, J., Flagan, R.C., Hansel, A., Möhler, O., Petäjä, T., Volkamer, R., Kulmala, M., Lehtipalo, K., Rissanen, M., Kirkby, J., El-Haddad, I., Bianchi, F., Sipilä, M., Donahue, N.M., Worsnop, D.R., 2022. High gas-phase methane sulfonic acid production in the OH-initiated oxidation of dimethyl sulfideat low temperatures. Environ. Sci. Technol. 56 (19), 13931–13944.

Stefels, J., Steinke, M., Turner, S., Malin, G., Belviso, S., 2007. Environmental constraints on the production and removal of the climatically active gas dimethylsulphide (DMS) and implications for ecosystem modelling. Biogeochemistry 83, 245–275.

Stein, A.F., Draxler, R.R., Rolph, G.D., Stunder, B.J.B., Cohen, M.D., Ngan, F., 2015. NOAA's HYSPLIT atmospheric transport and dispersion modeling system. BAMS 96, 2059–2077.

van Pinxteren, M., Fiedler, B., van Pinxteren, D., Iinuma, Y., Körtzinger, A., Herrmann, H. c., 2015. Chemical characterization of submicrometer aerosol particles in the tropical Atlantic Ocean: marine and biomass burning influen. J. Atmos. Chem. 72 (2), 105–125.

Veresa, P.R., Neuman, J.A., Bertram, T.H., Assaf, E., Wolfe, G.M., Williamson, C.J., Weinzierl, B., Tilmes, S., Thompson, C.R., Thames, A.B., Schroder, J.C., Saiz-Lopez, A., Rollins, A.W., Roberts, J.M., Price, D., Peischl, J., Nault, B.A., Møller, K.H., Miller, D.O., Meinardi, S., Li, Q., Lamarque, J.-F., Kupc, A., Kjaergaard, H.G., Kinnison, D., Jimene, J.L., Jernigan, C.M., Hornbrook, R.S., Hills, A., Dollner, M., Day, D.A., Cuevas, C.A., Campuzano-Jost, P., Burkholder, J., PaulBui, T., Brune, W. H., Brown, S., Brock, C.A., Bourgeois, I., DonaldR, Blake, Apel, E.C., Ryerson, T.B., 2020. Global airborne sampling reveals a previously unobserved dimethyl sulfide oxidation mechanism in the marine atmosphere. Proc. Natl. Acad. Sci. USA 117, 4505–4510.

Xu, J., Sun, J., Ren, J., Qin, D., 2005. Soluble species in the aerosols collected on the route of the second Chinese national arctic research expedition. J. Geophys. Res. 27 (2), 205–212.

Yang, X., Cox, R.A., Warwick, N.J., Pyle, J.A., Carver, G.D., O'Connor, F.M., Savage, N. H., 2005. Tropospheric bromine chemistry and its impacts on ozone: a modelstudy. J. Geophys. Res. 110, 1–18.

Zhang, Y., Wang, Y., Gray, B.A., Gu, D., Mauldin, L., Cantrell, C., Bandy, A., 2014. Surface and free tropospheric sources of methanesulfonic acid over the tropical Pacific Ocean. Geophys. Res. Lett. 41, 5239–5245.

Zhang, Y., Wang, Y., Zhang, X., Shen, X., Sun, J., Wu, L., Zhang, Z., Che, H., 2018. Chemical components, variation, and source identification of PM1 during heavy air pollution episodes in Beijing. J. Meteor. Res. 32 (1), 1–13.

Zhang, Y., Zhang, X., Zhong, J., Sun, J., Shen, X., Zhang, Z., Xu, W., Wang, Y., Liang, L., Liu, Y., Hu, X., He, M., Pang, Y., Zhao, H., Ren, S., Shi, Z., 2022. On the fossil and non-fossil fuel sources of carbonaceous aerosol with radiocarbon and AMS-PMF methods during winter hazy days in a rural area of North China plain. Environ. Res. 208, 112672.

Zorn, S.R., Drewnick, F., Schott, M., Hoffmann, T., Borrmann, S., 2008. Characterization of the South Atlantic marine boundary layer aerosol using an aerodyne aerosol mass spectrometer. Atmos. Chem. Phys. 8, 4711–4728.